Cation Exchange-Based Facile Aqueous Synthesis of Small, Stable, and Non-Toxic Near-Infrared Ag2Te/ZnS Core/Shell Quantum Dots Emitting in the Second Biological Window.

ARTICLE *in* ACS APPLIED MATERIALS & INTERFACES · JANUARY 2013

Impact Factor: 6.72 · DOI: 10.1021/am302933x · Source: PubMed

4 AUTHORS, INCLUDING:

Chi Chen
Chinese Academy of Sciences
10 PUBLICATIONS **54** CITATIONS
SEE PROFILE

Nan Ma
Soochow University (PRC)
25 PUBLICATIONS **579** CITATIONS
SEE PROFILE

ACS APPLIED MATERIALS & INTERFACES

Research Article

www.acsami.org

Cation Exchange-Based Facile Aqueous Synthesis of Small, Stable, and Nontoxic Near-Infrared Ag_2Te/ZnS Core/Shell Quantum Dots Emitting in the Second Biological Window

Chi Chen,[‡] Xuewen He,[†] Li Gao,[†] and Nan Ma*[,†,‡]

[†]The Key Lab of Health Chemistry and Molecular Diagnosis of Suzhou, College of Chemistry, Chemical Engineering and Materials Science, Soochow University, Suzhou, 215123, P. R. China

[‡]CAS Key Laboratory of Health Informatics, Shenzhen Institutes of Advanced Technology, Chinese Academy of Sciences, Shenzhen, 518055, P. R. China

Supporting Information

ABSTRACT: Facile aqueous synthesis of near-infrared Ag_2Te quantum dots (QDs) and Ag_2Te/ZnS core/shell QDs emitting in the second biological window is reported. The QD synthesis is based on a straightforward cation exchange process between CdTe QDs and Ag^+ ions conducted in aqueous solution. The prepared Ag_2Te QDs possess near-infrared emission ranging from 900 to 1300 nm and a quantum yield up to 2.1%. A ZnS shell was grown on the Ag_2Te QD to further enhance the photoluminescence intensity with a quantum yield of 5.6%. These Ag_2Te/ZnS core/shell QDs possess robust colloidal stability and photostability with minimum photoluminescence fluctuation upon incubation for 72 h in biological buffer or continuous laser excitation for 120 min. Also, These QDs possess small hydrodynamic size (~7.6 nm) and are non-cytotoxic to human cells, which is ideal for optical bioimaging in the second biological window.

KEYWORDS: *quantum dot, near-infrared, cation exchange, bioimaging, photoluminescence, silver chalcogenide*

INTRODUCTION

Quantum dots (QDs) are powerful bioimaging tools with exceptional optical properties including strong photoluminescence, robust photostability, tunable emission spectra, and broad absorption spectra that outperform the conventional organic fluorophores.[1−4] Near-infrared (NIR) light possesses much higher tissue penetration capability than visible light and is superior for in vivo optical imaging.[5−10] Recent studies showed that the NIR light within the second biological window (1000−1350 nm) could provide much higher signal-to-noise ratio and imaging depth than that within the first biological window (700−950 nm) due to the substantial reduction of tissue autofluorescence and scattering.[11,12] However, conventional NIR QDs are composed of toxic elements such as cadmium (Cd), lead (Pb), and mercury (Hg) which could cause potential long-term toxicity upon QD decomposition inside the body.[13,14] Silver (Ag)-based binary semiconductor QDs do not contain highly toxic components and hence are very promising for in vivo imaging. So far only a few synthetic strategies have been developed for silver-based QDs emitting in the second biological window, and all of these strategies are based on the high-temperature organometallic routes that require complexed precursors and stringent reaction conditions.[15−17] In addition, the QDs prepared in organic phase need to be further solubilized in aqueous solution during which QDs photoluminescence and stability can be drastically compromised. Therefore, a much-simplified and robust synthetic strategy to prepare water-soluble and stable Ag-based QDs for in vivo imaging is highly desirable.

Aqueous QDs synthesis represents an alternative strategy to the conventional organometallic routes and has been routinely adopted to prepare cadmium-based QDs emitting in the visible region.[18−22] Compared to the organometallic route, aqueous synthesis can be conducted under mild conditions and is much more straightforward. Moreover, the QDs prepared via aqueous synthesis are in general water-soluble, stable, and small in hydrodynamic size which are superior properties for bioimaging applications.[19,20] In this study we employed an aqueous solution-based cation exchange process to prepare luminescent Ag_2Te QDs with tunable emission wavelength within the second biological window. Highly efficient and fast cation exchange has been previously observed for cadmium-based nanocrystals (e.g. CdS, CdSe, and CdTe nanocrytals) with Ag^+ ions to form cognate silver-based nanocrystals in organic phase,[23] whereas the as-prepared materials do not exhibit photoluminescence. Herein, we establish a facile strategy for aqueous synthesis of luminescent silver-based QDs by coupling the aqueous synthesis of cadmium-based QDs with the subsequent QD cation exchange with Ag^+ ions (Scheme 1).

Received: December 2, 2012
Accepted: January 16, 2013
Published: January 16, 2013

   dx.doi.org/10.1021/am302933x | *ACS Appl. Mater. Interfaces* 2013, 5, 1149−1155

Scheme 1. Schematic Illustration of the Aqueous Synthesis of Ag_2Te QDs and Ag_2Te/ZnS Core/Shell QDs Based on Cation Exchange of CdTe QDs with Ag^+ Ions

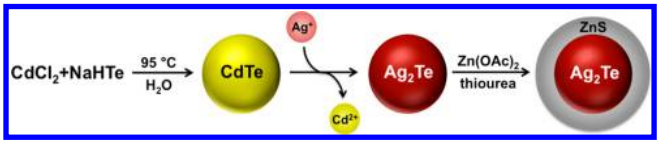

EXPERIMENTAL SECTION

Materials and Instrumentations. Silver nitrate ($AgNO_3$, >99.9%), cadmium chloride ($CdCl_2$, 99.996%), tellurium powder (Te, 60-mesh, 99.999%) and thiourea (≥99%) were purchased from Alfa Aesar. Zinc acetate ($Zn(OAc)_2$, 99.99%), glutathione (GSH, ≥98%), and sodium borohydride ($NaBH_4$, ≥99%) were purchased from Sigma-Aldrich. Water was purified with a Milli-Q water purification system. All other reagents and solvents were of analytical grade. The fluorescence spectra and absorption spectra were recorded on a FSP 920 fluorometer and a PerkinElmer Lambda 25 absorption spectrophotometer respectively. Transmission electron microscopy

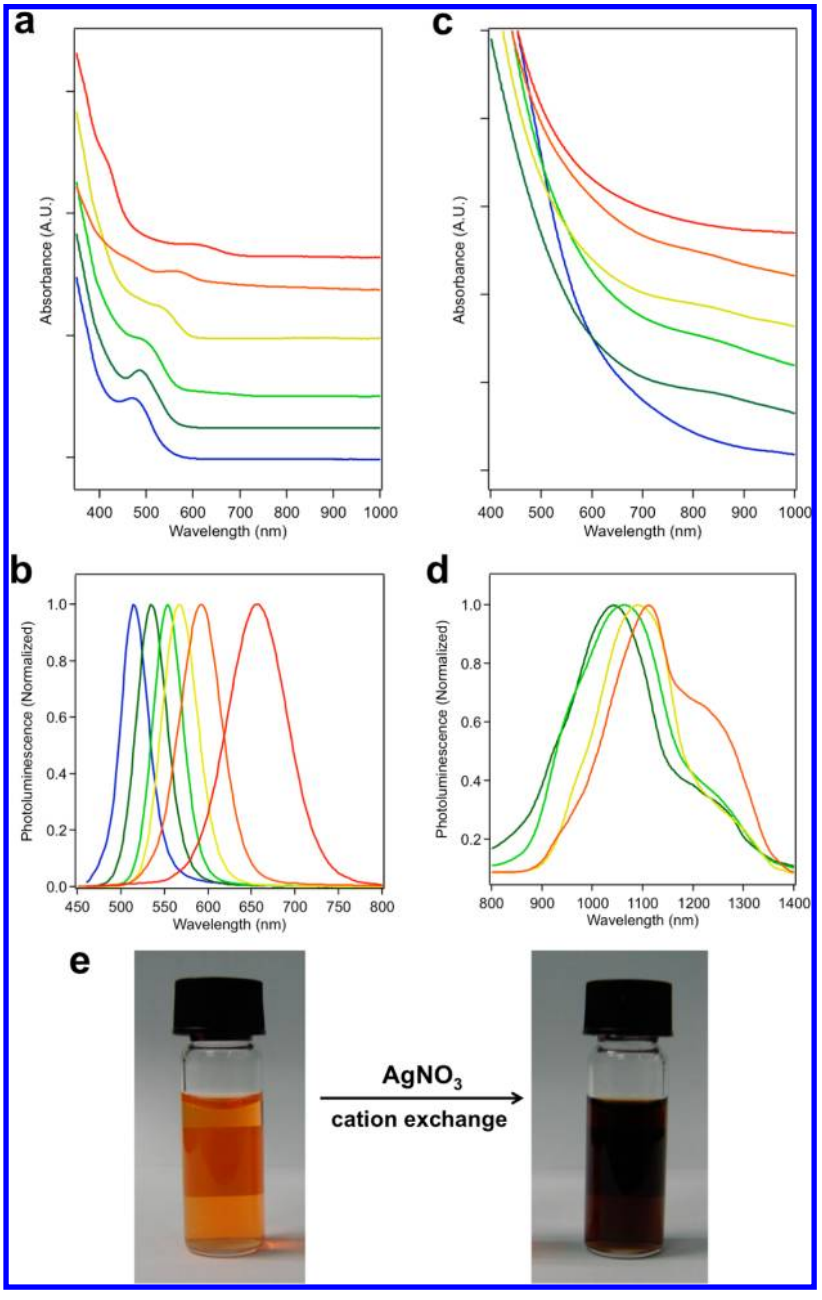

Figure 1. Optical characterization of CdTe QDs and Ag_2Te QDs. (a) Absorption spectra of CdTe QDs synthesized with various reaction time (from bottom to top: 15, 30, 45, 60, 90, and 150 min). (b) Photoluminescence spectra of CdTe QDs synthesized with various reaction time (from left to right: 15, 30, 45, 60, 90, and 150 min). (c) Absorption spectra of Ag_2Te QDs prepared from CdTe QDs via cation exchange (The corresponding CdTe QDs and Ag_2Te QDs are depicted in the same color). (d) Photoluminescence spectra of Ag_2Te QDs prepared from CdTe QDs via cation exchange (The corresponding CdTe QDs and Ag_2Te QDs are depicted in the same color). The cation exchange products prepared from the smallest and biggest CdTe QDs are not luminescent and not shown in the figure. (e) Photographs of the CdTe QDs (left) and the Ag_2Te QDs (right) prepared via cation exchange. (A rectangular label attached to the back of the bottle can be visualized through the CdTe QDs solution (left).).

dx.doi.org/10.1021/am302933x | ACS Appl. Mater. Interfaces 2013, 5, 1149−1155

(TEM) images and energy dispersive X-rays (EDXs) were taken on a FEI Tecnai G2 F20 S-Twin transmission electron microscope operating at 200 kV. Hydrodynamic size distribution was measured on a Malvern Zetasizer Nano ZS analyzer. X-ray diffraction (XRD) measurements were performed on a PANalytical X'pert PRO Multiple Crystals (powder) X-ray Diffractometer. Elemental analysis of QDs was performed on a ICP-AES spectrometer (Varian 710-ES) after nitric acid treatment of the sample.

Synthesis and Characterization of CdTe, Ag_2Te, and Ag_2Te/ZnS QDs. Sodium hydrogen tellurium (NaHTe) was freshly made before each synthesis by dissolving 0.0400 g sodium borohydride ($NaBH_4$) in 1.0 mL deionized water and then 0.0638 g tellurium powder was added into the $NaBH_4$ solution. This reaction was conducted in an ice bath for 8 h. $CdCl_2$ stock solution was prepared by dissolving 0.0915 g $CdCl_2$ in 10 mL water. $AgNO_3$ stock solution was prepared by dissolving 0.0339 g $AgNO_3$ in 1 mL water. $Zn(OAc)_2$ stock solution was prepared by dissolving 0.183 g $Zn(OAc)_2$ in 10 mL water. The GSH stabilizer solution was prepared by dissolving 0.123 g GSH in 10 mL water. The thiourea stock solution was prepared by dissolving 0.0761 g thiourea in 10 mL water. For CdTe QD synthesis, the cadmium/GSH/tellurium molar ratio was set to 1:1.6:0.5. For a 10 mL synthesis, 0.5 mL $CdCl_2$ (0.05 M) and 1.0 mL GSH (0.04 M) were added to a 50 mL centrifuge tube and diluted to 10 mL with water, and the pH of the solution was adjusted to 11.0 by dropwise addition of 1.0 M NaOH solution while stirring. After degassed for 15 min with argon, 25 μL of as-prepared NaHTe (0.5 M) was injected into the above mixture solution. This solution was then incubated on a heat block preheated to 95 °C for 15, 30, 45, 60, 90, and 150 min to promote nanocrystal growth. This procedure was repeated for more synthesis. To obtain Ag_2Te QDs, 12.5 μL of $AgNO_3$ (0.2 M) and 1 mL of CdTe QDs with different sizes (1.27, 1.84, 2.98, 3.30, 3.66, or 3.75 nm) were added into a 1.5 mL Eppendorf tube to promote the cation exchange process, and the photoluminescence (λ_{ex} = 400 nm) of Ag_2Te QDs was recorded immediately. To synthesize Ag_2Te/ZnS (core/shell) QDs, the prepared Ag_2Te QDs were first purified with a MicrosepAdvance Centrifugal Device (YM-3, Pall Corporation) via centrifugation at 8000 rpm for 15 min, and then, the QDs were recovered in the same volume of H_2O. A 200 μL portion of purified Ag_2Te QDs (2.34 nm), 2.5 μL of $Zn(Ac)_2$ (0.1 M), and 1.25 μL of thiourea (0.1 M) were loaded into a 1.5 mL Eppendorf tube. The solution was then incubated on a heat block preheated to 75 °C for 1 h and the QDs photoluminescence (λ_{ex} = 400 nm) was recorded. The quantum yields (QYs) of the QDs were calculated according to the following equation:

$$\Phi_x = \Phi_s[A_s/A_x][\mathrm{Int}_x/\mathrm{Int}_s][\eta_x/\eta_s]^2$$

Where, Φ is the quantum yield, A is absorbance at the excitation wavelength, Int is the area under the emission peak, and η is the refractive index of the solvent. The subscripts s and x denote the respective values of the standard and QDs. Rhodamine 6G (QY = 95% in methanol) was used as a standard for CdTe QDs. Dye 26 (QY = 0.5% in 1,2-dichloroethane) was used as a standard for Ag_2Te and Ag_2Te/ZnS QDs.

Stability Measurements. To measure the colloidal stability of Ag_2Te/ZnS (core/shell) QDs, the QDs (1 μM) were incubated in water, 1× PBS, or fetal bovine serum at 37 °C, and the photoluminescence intensity of the QDs was recorded at different time points (0, 4, 8, 12, 24, 36, 48, and 72 h). To measure the photostability of Ag_2Te and Ag_2Te/ZnS (core/shell) QDs, the QDs (1 μM) in water were excited continuously with a 405 nm laser (50 mW) and the photoluminescence intensity of the QDs was recorded at different time points (0, 15, 30, 45, 60, 75, 90, 105, 120 min). To measure the photostability of the indocyanine green (ICG) molecules, ICG (1 μM) in water were excited continuously with a 722 nm laser (50 mW) and the photoluminescence intensity of ICG was recorded at different time points (0, 15, 30, 45, 60, 75, 90, 105, 120 min).

Cytotoxicity Measurements. HeLa cells were cultured as subconfluent monolayers on 25 cm^2 cell culture plates with vent caps (Corning) in 1× minimum essential α medium (Gibco) supplemented with 10% fetal bovine serum (Hyclone) in a humidified incubator at 37 °C containing CO_2 (5%). HeLa cells that had been grown to subconfluence were dissociated from the surface with a solution of 0.25% trypsin/EDTA (Hyclone) for 30 s at 37 °C, and aliquots (100 μL) were seeded (2 ×10^4 cells) into a 96-well plate (Costar). After overnight incubation, the medium was replaced with 100 μL serum-free MEM medium containing 100 nM Ag_2Te/ZnS QDs or Ag_2Te QDs (1:10 dilution of 1 μM QDs in water). Cells were incubated in the dark at 37 °C for 6, 12, 18, and 24 h. Cells treated with media alone and Triton X-100 were used as low and high cell death controls, respectively. Cell viabilities were then quantitated using a standard MTT assay.

RESULTS AND DISCUSSION

In order to synthesize Ag_2Te QDs, CdTe QDs were used as the QD precursor for cation exchange. Bulk Ag_2Te semiconductors

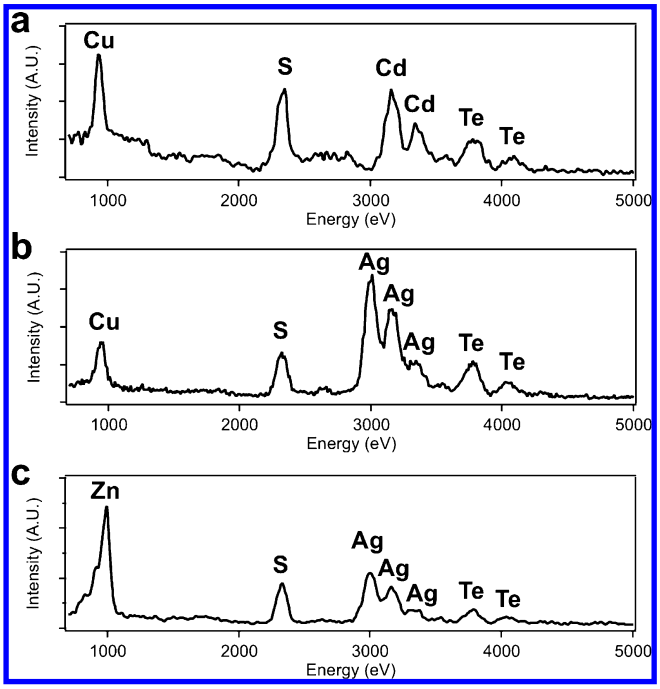

Figure 2. EDX characterization of (a) CdTe QDs, (b) Ag_2Te QDs, and (c) Ag_2Te/ZnS core/shell QDs.

with low temperature monoclinic β-phase has an optical energy gap of 0.67 eV, and the emission wavelength of the corresponding Ag_2Te QDs are expected to fall into the second biological window. CdTe QDs were synthesized in H_2O according to a previously reported protocol.[24] Briefly, $CdCl_2$ and NaHTe were used as QD precursors and glutathione (GSH) was used as ligands. The reaction was conducted at 95 °C for different time (15, 30, 45, 60, 90, and 150 min) to obtain CdTe QDs with various sizes and emission wavelengths. As shown in Figure 1a and c, both the first absorption peak and the band-edge emission maximum shifted to longer wavelength with increased reaction time as a result of CdTe QD growth. The quantum yield (QY) of the prepared CdTe QDs was dependent on the size of the QDs. A highest QY of 32% was achieved for the CdTe QDs with an emission maximum of 554 nm. To obtain Ag_2Te QDs, cation exchange of different sized CdTe QDs with Ag^+ ions was conducted in aqueous solution. $AgNO_3$ solution with a Ag to Te molar ratio of 2:1 was introduced to the CdTe QDs solution and the QDs solution color changed from orange to dark brown instantaneously

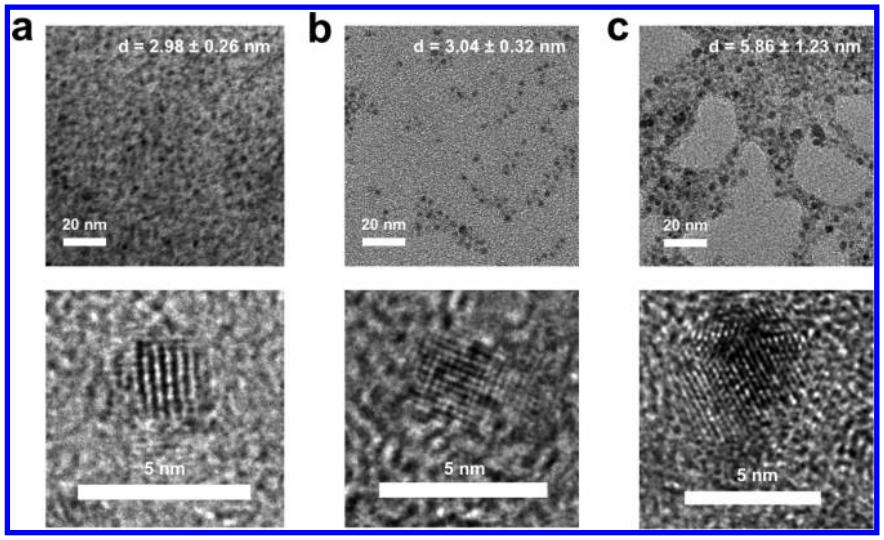

Figure 3. Low magnification (top) and high-resolution (bottom) TEM images of (a) CdTe QDs, (b) Ag_2Te QDs, and (c) Ag_2Te/ZnS core/shell QDs. (Scale bars are 20 nm in the top images and 5 nm in the bottom images.).

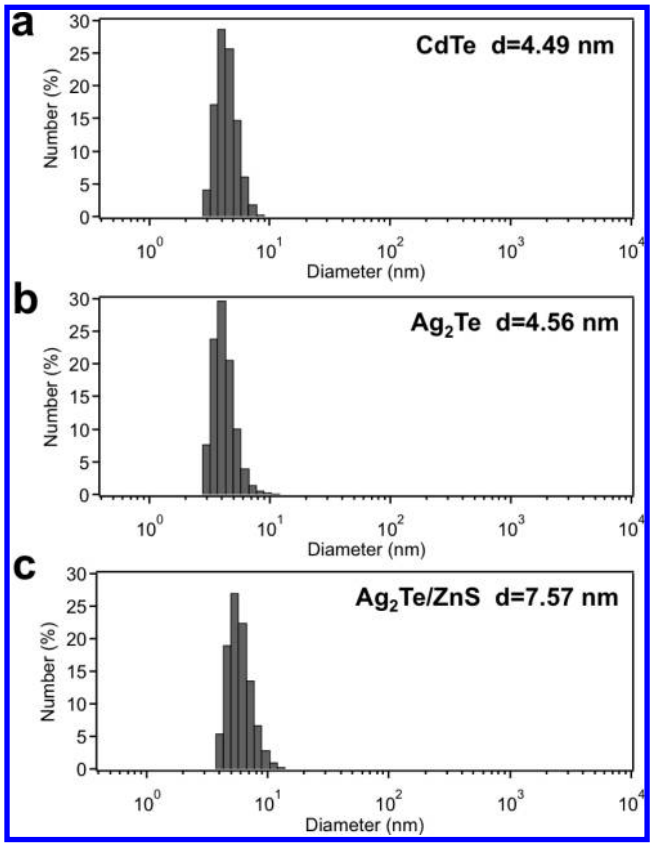

Figure 4. Hydrodynamic size distributions of (a) CdTe QDs, (b) Ag_2Te QDs, and (c) Ag2Te/ZnS QDs measured by DLS.

(Figure 1e), which indicates that the cation exchange proceeded very fast. The QD product was characterized by absorption and photoluminescence spectroscopy. As shown in Figure 1b, after reacting with Ag^+ ions, the absorption spectra of different sized CdTe QDs all extended to the NIR region, which implies the formation of QDs with smaller optical energy gaps. Similar transitions of absorption spectra were previously observed for the conversion of CdSe to Ag_2Se QDs via cation exchange proceeded in organic solvents.[23] Meanwhile, the CdTe photoluminescence all disappeared after cation exchange and NIR emission (~900 to ~1300 nm) was generated (Figure 1d), implying the transformation of CdTe QDs to NIR light-emitting QDs. It is noticeable that the photoluminescence properties of the QD products are highly dependent on the size of the original CdTe QD precursors. Among the six different sized CdTe QDs precursors used for cation exchange, the smallest and the largest QDs (e.m. = 514 and 656 nm) did not produce luminescent products whereas the other four CdTe QDs precursors (e.m. = 534, 554, 566, and 594 nm) lead to the formation of NIR light-emitting QDs (Figure 1d). The quenched photoluminescence for the smallest and largest QDs is likely due to the defects introduced to the nanocrystals during cation exchange. In addition, there is a shift of the emission maximum to longer wavelength (from 1042 to 1120 nm) for the NIR QDs products prepared from the CdTe QDs precursors with increasing sizes (Figure 1d). The photoluminescence spectra of the QD products exhibited a shoulder to the red of the major emission peak which is likely due to the trap state emission given that no agglomeration was detected for Ag_2Te QDs (Figure 1d). A highest QY (2.1%) was achieved for the Ag_2Te QDs prepared from the CdTe QDs with an emission maximum of 554 nm. Relatively low QYs of silver chalcogenide QDs (e.g. Ag_2Se QDs) have been commonly observed in other studies,[16,25] which may be attributed to the inherent properties of Ag-based semiconductor nanocrystals. A previous study showed that the Ag_2Te QDs with a diameter of 3.2 nm prepared in organic solvents exhibit an emission peak at 1300 nm, whereas the QY is not reported.[16] The elemental composition of the QDs before and after cation exchange was explored using energy-dispersive X-ray spectroscopy (EDX) (Figure 2). Before cation exchange cadmium and tellurium were identified as the QD components. After cation exchange and purification, silver and tellurium were identified as the QD components. Inductively coupled plasma atomic emission spectroscopy (ICP-AES) further confirms the absence of cadmium after cation exchange, suggesting the complete transformation of CdTe QDs to Ag_2Te QDs. Typical transmission electron microscopy (TEM) images of CdTe QDs (e.m. = 554 nm) and the corresponding Ag_2Te QDs (e.m. = 1060 nm) were shown in Figure 3. Numerous near monodisperse spherical nanoparticles can be observed in the

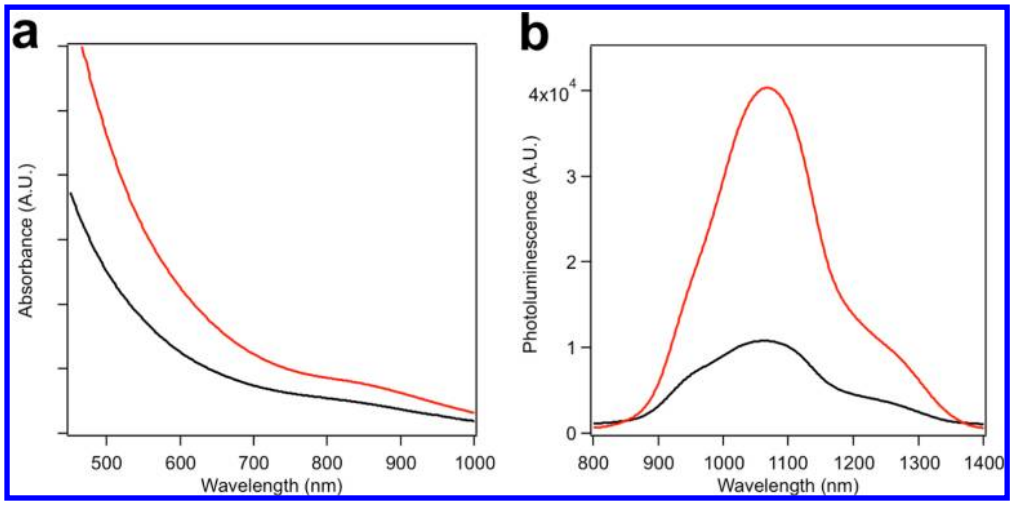

Figure 5. (a) Absorption spectra and (b) photoluminescence spectra of Ag_2Te QDs (black) and Ag_2Te/ZnS core/shell QDs (red).

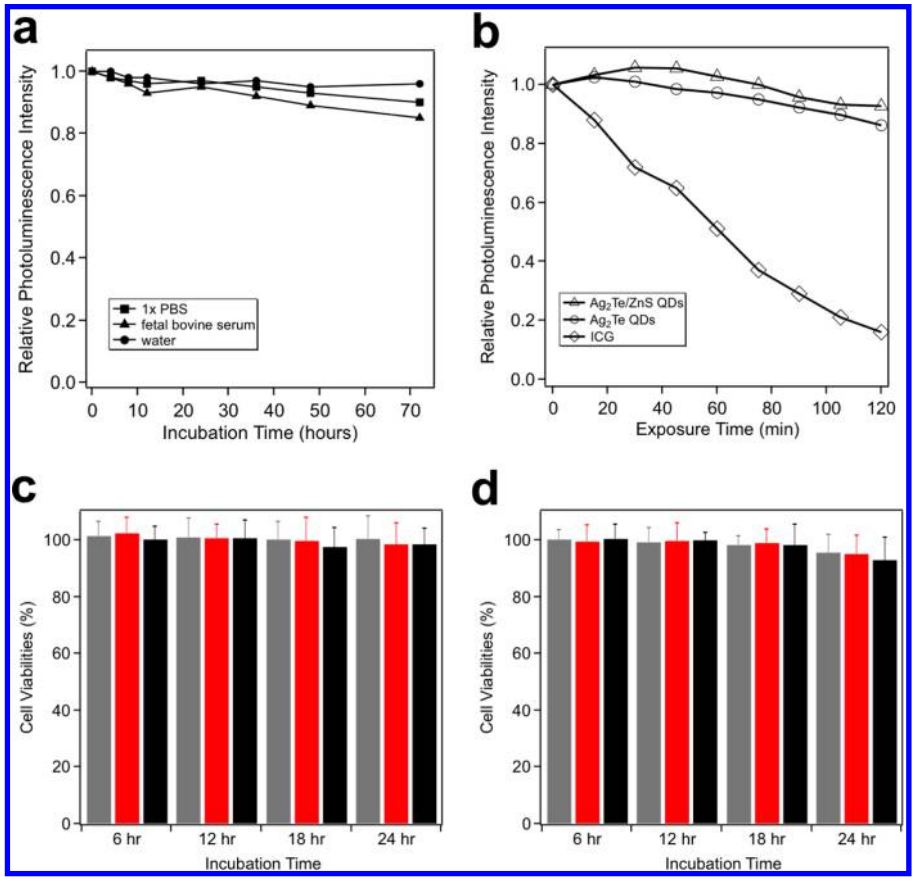

Figure 6. Stability and cytotoxicity measurements of Ag_2Te/ZnS core/shell QDs. (a) Colloidal stability of Ag_2Te/ZnS QDs in water, 1× PBS, and fetal bovine serum. (b) Photostability of Ag_2Te/ZnS QDs, Ag_2Te QDs, and ICG molecules in water. (c) Cell viability data of HeLa cells incubated with Ag_2Te/ZnS QDs (grey 50 nM; red 100 nM; black 200 nM). (d) Cell viability data of HeLa cells incubated with Ag_2Te QDs (grey 50 nM; red 100 nM; black 200 nM).

low-magnification images and the crystal lattice fringes can be identified in high-resolution images for both CdTe and Ag_2Te QDs. The mean diameter of the QDs before and after cation exchange are 2.98 ± 0.26 and 3.04 ± 0.32 nm according to TEM images. The hydrodynamic sizes of the CdTe and the corresponding Ag_2Te QDs were 4.49 and 4.56 nm, respectively, determined using dynamic light scattering (DLS) (Figure 4). The powder X-ray diffraction (XRD) pattern of the Ag_2Te QDs agrees mostly with the low temperature monoclinic β-phase of Ag_2Te (JCPDS 81-1820) (Supporting Information Figure S1). Significant peak broadening was observed due to the tiny size of QD nanocrystals. In order to further enhance the photoluminescence intensity of the prepared Ag_2Te QDs, we sought to grow a ZnS shell on the Ag_2Te QD to achieve better surface passivation. Ag_2Te QDs with highest QY were used for the construction of Ag_2Te/ZnS core/shell QDs. Briefly, the Ag_2Te QDs were first purified using a Microsep Advance Centrifugal Device (YM-3) to remove all the free Cd^{2+} ions and ligand

molecules after which $Zn(Ac)_2$ and thiourea were introduced to the QDs solution and reacted at 75 °C for 1 h. The QY increased to 5.6% after shell growth and the emission maximum remain unchanged (Figure 5). It is noteworthy that the QY of the prepared Ag_2Te/ZnS core/shell QDs is much higher than that of the commonly used NIR organic fluorophore—indocyanine green (ICG, QY = 1.3%). The mean diameter of nanocrystals increased to 5.86 ± 1.23 nm after shell formation according the TEM image (Figure 3c). The hydrodynamic size also increased from 4.56 to 7.57 nm according to DLS measurements (Figure 4c). EDX experiment confirms the presence of zinc elements after shell growth (Figure 2c).

The colloidal stability of the prepared Ag_2Te/ZnS core/shell QDs was evaluated by incubating the QDs in water, 1× PBS, and fetal bovine serum at 37 °C, respectively, and the photoluminescence intensity was recorded at different time points. As shown in Figure 6a, up to 90% of photoluminescence was preserved after 72 h incubation, suggesting that these QDs are highly stable for bioimaging applications. The photostabilities of the Ag_2Te QDs and Ag_2Te/ZnS core/shell QDs were evaluated by continuously exciting the QDs with a 405 nm laser (50 mW). As shown in Figure 6b, little photobleaching was observed after continuous excitation of QDs for up to 120 min, revealing the high capacity of these QDs for long-term imaging and tracking. In contrast, significant photobleaching of ICG was observed under continuous excitation with a 722 nm laser (50 mW) (Figure 6b). The cytotoxicities of the prepared Ag_2Te/ZnS QDs and Ag_2Te QDs were tested with HeLa cells using MTT assay. Negligible effects on cell viabilities were observed after 24 h incubation of HeLa cells with the two types of QDs under various QDs concentrations (50, 100, 200 nM) (Figure 6c and 6d).

CONCLUSIONS

In conclusion, we report a new strategy to synthesize Ag_2Te QDs and Ag_2Te/ZnS core/shell QDs emitting in the second biological window. The entire synthesis was conducted in aqueous solution without any complexed precursors and stringent reaction conditions, which is much more facile in comparison with the previously reported organometallic synthetic routes. Syntheses of Ag_2Te nanostructures have been previously reported in several studies and cation exchange-based production of Ag_2Te nanowires in aqueous solution was reported.[26−30] However, most of the as-prepared materials are nonluminescent. So far the only successful synthesis of luminescence Ag_2Te QDs was conducted in organic phase via an organometallic route.[16] To the best of our knowledge, our work is the first one to synthesize luminescent Ag_2Te QDs via cation exchange in aqueous solution. The prepared QDs possess small hydrodynamic sizes, robust colloidal stability and photostability, and are nontoxic to human cells, which would be ideal for bioimaging applications.

ASSOCIATED CONTENT

Supporting Information

Figure S1. This material is available free of charge via the Internet at http://pubs.acs.org.

AUTHOR INFORMATION

Corresponding Author

*E-mail: nan.ma@suda.edu.cn.

Notes

The authors declare no competing financial interest.

ACKNOWLEDGMENTS

This work was supported in part by National Science Foundation of China (21175147), the Recruitment Program of Global Young Experts (1000-Young Talents Plan), the Project of Scientific and Technologic Infrastructure of Suzhou (SZS201207), and startup funds from Soochow University.

REFERENCES

(1) Alivisatos, A. P. *Science* **1996**, *271*, 933−937.
(2) Chan, W. C. W.; Nie, S. *Science* **1998**, *281*, 2016−2018.
(3) Michalet, X.; Pinaud, F. F.; Bentolila, L. A.; Tsay, J. M.; Doose, S.; Li, J. J.; Sundaresan, G.; Wu, A. M.; Gambhir, S. S.; Weiss, S. *Science* **2005**, *307*, 538−544.
(4) Medintz, I. L.; Uyeda, H. T.; Goldman, E. R.; Mattoussi, H. *Nature Mater* **2005**, *4*, 435−446.
(5) Kim, S.; Lim, Y. T.; Soltesz, E. G.; De Grand, A. M.; Lee, J.; Nakayama, A.; Parker, J. A.; Mihaljevic, T.; Laurence, R. G.; Dor, D. M.; Cohn, L. H.; Bawendi, M. G.; Frangioni, J. V. *Nat. Biotechnol.* **2004**, *22*, 93−97.
(6) Bentolila, L. A.; Ebenstein, Y.; Weiss, S. *J. Nucl. Med.* **2009**, *50*, 493−496.
(7) He, Y.; Zhong, Y.; Su, Y.; Lu, Y.; Jiang, Z.; Peng, F.; Xu, T.; Su, S.; Huang, Q.; Fan, C.; Lee, S.-T. *Angew. Chem. Int. Ed.* **2011**, *50*, 5695−5698.
(8) Yong, K. T.; Roy, I.; Ding, H.; Bergey, E. J.; Prasad, P. N. *Small* **2009**, *5*, 1997−2004.
(9) Gao, J.; Chen, K.; Luong, R.; Bouley, D. M.; Mao, H.; Qiao, T.; Gambhir, S. S.; Cheng, Z. *Nano Lett.* **2012**, *12*, 281−286.
(10) Morgan, N. Y.; English, S.; Chen, W.; Chernomordik, V.; Russo, A.; Smith, P. D.; Gandjbakhche, A. *Acad. Radiol.* **2005**, *12*, 313−323.
(11) Smith, A. M.; Mancini, M. C.; Nie, S. *Nat. Nanotechnol.* **2009**, *4*, 710−711.
(12) Welsher, K.; Liu, Z.; Sherlock, S. P.; Robinson, J. T.; Chen, Z.; Daranciang, D.; Dai, H. *Nat. Nanotechnol.* **2009**, *4*, 773−780.
(13) Hinds, S.; Myrskog, S.; Levina, L.; Koleilat, G.; Yang, J.; Kelley, S. O.; Sargent, E. H. *J. Am. Chem. Soc.* **2007**, *129*, 7218−7219.
(14) Qian, H.; Dong, C.; Peng, J.; Qiu, X.; Xu, Y.; Ren, J. *J. Phys. Chem. C.* **2007**, *111*, 16852−16857.
(15) Sahu, A.; Qi, L.; Kang, M.-S.; Deng, D.; Norris, D. J. *J. Am. Chem. Soc.* **2011**, *133*, 6509−6512.
(16) Yarema, M.; Pichler, S.; Sytnyk, M.; Seyrkammer, R.; Lechner, R. T.; Fritz-Popovski, G.; Jarzab, D.; Szendrei, K.; Resel, R.; Korovyanko, O.; Loi, M. A.; Paris, O.; Hesser, G.; Heiss, W. *ACS Nano* **2011**, *5*, 3758−3765.
(17) Du, Y.; Xu, B.; Fu, T.; Cai, M.; Li, F.; Zhang, Y.; Wang, Q. *J. Am. Chem. Soc.* **2010**, *132*, 1470−1471.
(18) Zheng, Y.; Gao, S.; Ying, J. Y. *Adv. Mater.* **2007**, *19*, 376−380.
(19) Ma, N.; Sargent, E. H.; Kelley, S. O. *Nat. Nanotechnol.* **2009**, *4*, 121−125.
(20) Law, W. C.; Yong, K. T.; Roy, I.; Ding, H.; Hu, R.; Zhao, W.; Prasad, P. N. *Small* **2009**, *5*, 1302−1310.
(21) Aldeek, F.; Balan, L.; Medjahdi, G.; Roques-Carmes, T.; Malval, J.-P.; Mustin, C.; Ghanbaja, J.; Schneider, R. *J. Phys. Chem. C* **2009**, *113*, 19458−19467.
(22) Rogach, A. L.; Franzl, T.; Klar, T. A.; Feldmann, J.; Gaponik, N.; Lesnyak, V.; Shavel, A.; Eychmüller, A.; Rakovich, Y. P.; Donegan, J. F. *J. Phys. Chem. C* **2007**, *111*, 14628−14637.
(23) Son, D. H.; Hughes, S. M.; Yin, Y.; Alivisatos, A. P. *Science* **2004**, *306*, 1009−1012.
(24) Qian, H.; Dong, C.; Weng, J.; Ren, J. *Small* **2006**, *2*, 747−751.
(25) Gu, Y.-P.; Cui, R.; Zhang, Z.-L.; Xie, Z.-X.; Pang, D.-W. *J. Am. Chem. Soc.* **2012**, *134*, 79−82.
(26) Taniguchi, S.; Green, M. *J. Mater. Chem.* **2011**, *21*, 11592−11598.

(27) Liu, Y.-W.; Ko, D.-K.; Oh, S. J.; Gordon, T. R.; Doan-Nguyen, V.; Paik, T.; Kang, Y.; Ye, X.; Jin, L.; Kagan, C. R.; Murray, C. B. *Chem. Mater* **2011**, *23*, 4657−4659.
(28) Samal, A. K.; Pradeep, T. *J. Phys. Chem. C.* **2009**, *113*, 13539−13544.
(29) Qin, A.; Fang, Y.; Tao, P.; Zhang, J.; Su, C. *Inorg. Chem.* **2007**, *46*, 7403−7409.
(30) Tang, Z.; Podsiadlo, P.; Shim, B. S.; Lee, J.; Kotov, N. A. *Adv. Funct. Mater* **2008**, *18*, 3801−3808.